Chemical Physics Letters 563 (2013) 25–29

Contents lists available at SciVerse ScienceDirect

Chemical Physics Letters

journal homepage: www.elsevier.com/locate/cplett

Towards energy decomposition analysis for open and closed shell f-elements mono aqua complexes

A. Marjolin [a,b], C. Gourlaouen [c], C. Clavaguéra [d], J.-P. Dognon [a], J.-P. Piquemal [b,*]

[a] Laboratoire de Chimie de Coordination des Eléments-f, CEA, CNRS UMR 3299, CEA Saclay, 91191 Gif-sur Yvette Cedex, France
[b] Laboratoire de Chimie Théorique, UPMC, CNRS UMR 7616, CC 137, 4 Place Jussieu, 75252 Paris Cedex 05, France
[c] Laboratoire de Chimie Quantique, Université de Strasbourg, CNRS UMR 7177, PB 296 1 Rue Blaise Pascal, 67008 Strasbourg Cedex, France
[d] Laboratoire des Mécanismes Réactionnels, Département de Chimie, Ecole Polytechnique, CNRS, 91 128 Palaiseau Cedex, France

ARTICLE INFO

Article history:
Received 17 November 2012
In final form 31 January 2013
Available online 8 February 2013

ABSTRACT

We propose an energy decomposition analysis of mono aqua systems of both open and closed shell lanthanide and actinide cations using the CSOV scheme. We compared the values obtained with either large f-in-core or small core quasi relativistic pseudopotentials and computed the unpaired electrons contribution to the polarization energy component. Through a quasi-systematic approach on a number of chosen f-element cations, we quantified the different trends across both series for each contribution. This work is an important preliminary step for the acquisition of reference ab initio data for further parameterization of polarizable force fields for lanthanides and actinides.

1. Introduction

Lanthanides (Ln) and Actinides (An) form a block of elements called the f-elements because of the presence of either 4f or 5f orbitals respectively. They respectively have a [Xe] $5d^1$ $6s^2$ $4f^n$ and [Rn] $6d^1$ $7s^2$ $5f^n$ configuration (n = 1–14). The different cations are then formed by losing first the s- and d-electrons then the f-electrons. Completely filled or empty f-orbitals will therefore lead to closed shell cations, while partially filled orbitals will generate multi reference open shell systems. Having the same outermost shell configuration, the elements from those two lines often exhibit very similar chemical behavior, more specifically in the case of trivalent cations. This oxidation state is the most common one for the elements of the lanthanide series and for the transplutonium elements of the actinide series such as Am(III) or Cm(III). In many ways, lanthanide and actinide ions resemble the alkaline earth ions since they are often described as hard acids with a strong preference for oxygen donor ligands, the simplest of which is water. However, in particular cases, Ln and An cations undergo selective complexation with particular ligands. Such complexation phenomena have direct applications in medical diagnosis as contrast agents in magnetic resonance imaging or luminescent probes for proteins [1–3], in synthesis [4] but also in nuclear waste management and nuclear toxicology studies [5–7]. A means to understand the preferential binding of heavy metals is through the study of the interaction energy between the metal cations and ligands, and of its physical components by means of quantum chemical approaches [8–11]. In this work, binding energies of both closed-shell and open-shell lanthanide and actinide cations with water will be addressed as the different physical interactions at play will be deconvoluted through the use of the constrained space orbital variation (CSOV) energy decomposition analysis approach (EDA) [12–14]. Such results would be of prime importance for the EDA based ab initio parameterization of the polarization contribution of new generation polarizable force fields [15–21]. We will focus on two different EDA strategies based on the use of both small and large core scalar relativistic pseudopotentials.

2. Procedure

2.1. EDA methodology

Energy decomposition analyses (EDA) are a useful tool to estimate the intermolecular interaction energies of metal–ligand systems. Also the separation into the different contributions to this interaction energy gives insight on the nature of the bond. Indeed the interaction energy of a dimer system consisting of monomers A and B can be calculated as the sum of different energy terms i.e. electrostatic interaction between the fragments (E_{elec}), exchange-repulsion linked to Pauli's repulsion between parallel spin electrons ($E_{exch\text{-}rep}$), the monomer polarization contribution (E_{pol}) due to the relaxation of a given fragment's occupied orbitals within its virtual orbitals in the field of another fragment, and the charge transfer term (E_{ct}) accounting for donation and back-donation.

$$E_{int} = E_{elec} + E_{exch-rep} + E_{pol} + E_{ct}$$

* Corresponding author.
E-mail addresses: jpp@lct.jussieu.fr, jean-philip.piquemal@upmc.fr (J.-P. Piquemal).

0009-2614/$ - see front matter © 2013 Elsevier B.V. All rights reserved.
http://dx.doi.org/10.1016/j.cplett.2013.01.066

The different contributions are evaluated by carrying out constrained SCF procedures in which specific orbitals are frozen. E_1 (or frozen core energy) denotes the sum of $E_{elec} + E_{exch-rep}$ and E_2 corresponds to the sum of $E_{pol} + E_{ct}$. Among the different methods available for such decomposition schemes, we chose the constrained space orbital variation (CSOV) method at the Hartree–Fock level to carry out our study. This choice was motivated by the need for a pure polarization energy contribution which will be further used for force field developments [15–21]. CSOV is based on the definition of a variational space from the isolated monomers' occupied and virtual orbitals. Please note that within the CSOV procedure, linear dependencies of the basis set are removed leading to slightly smaller active space and therefore to small differences with usual BSSE corrected interaction energies. Besides HF, DFT based decompositions are also implemented, in which case, the variational space is built using Kohn–Sham orbitals. However, even if some of the correlation can be recovered using density functional theory, we chose to stick to the HF method. Indeed, none of the actual popular DFT functionals are designed to specifically study f-elements and computational errors, also linked to the fact that most pseudopotentials are adjusted within wavefunction based schemes, can arise from their use. In the CSOV approach, the supermolecule wavefunction is kept antisymmetric, contrarily to the procedure developed by Kitaura and Morokuma [22] allowing a physical inclusion of exchange-polarization effects which is mandatory (see discussion on reference [14]). Note that no dispersion contribution is added at this uncorrelated (HF) level. Indeed, as we will see in Section 2.2, performing correlated MCSCF EDA computations generates difficulties.

2.2. Computational details

All energy decomposition calculations were carried out with a modified version of the Hondo95.3 code [23]. The geometries were previously calculated at MRCI level using the Molpro package [24].

For optimization we used the Dunning's augmented triple zeta basis sets for H and O [25] and Stuttgart–Cologne smallcore quasi-relativistic effective core potentials (RECPs) and associated basis sets for cations. In addition, for EDA, small and large core RECPs and associated basis sets were used for the cation [26–31]. The different complete active spaces (CAS) for the multi reference calculation are given in Table 1. Also all geometry optimizations were carried out in C_{2V} group and in the most stable symmetry of the wavefunction. The EDA was first carried out on the optimized geometry and the metal–ligand distance was then varied so as to obtain a curve of each of the contributions as a function of the inter fragment distance. The aug-cc-pVTZ basis set was kept for the water fragment but for the cations, calculations were carried out with both the small core pseudopotential and a large f-in-core pseudopotential. The basis set superposition error (BSSE) was evaluated using the counterpoise correction to less than 0.1% of the interaction energy at Hartree–Fock level and therefore considered negligible. The aim was to compare the general behavior of both pseudopotentials and assess the contribution of the unpaired electrons to the polarization energy in the case of the open shell systems. In the case of Eu(III), Eu(II), Gd(III), Am(III) and Cm(III) the use of f in-core pseudopotentials turned the open shell systems to a closed shell system of multiplicity 2S + 1 = 1. In all cases however the pseudopotentials had to be modified in such a way that the h-component was removed since it is not handled by the HONDO code. Each fragment had to be first calculated separately so as to generate the wavefunctions needed in the decomposition energy scheme for the super molecule. Explicit open-shell EDA computation using small core pseudopotentials have been handled following Bagus and Bauschlicher [13] by using MCSCF wavefunctions obtained with the complete active space approach (CASSCF). In this approach, the active electrons correspond to the unpaired f-electrons only. Such a choice is made in order to produce uncorrelated 'Hartree–Fock like' computations. Here, the CASSCF approach is a technical means enabling a convenient handling of unpaired electrons thanks to the possibility of having single orbital occupancies [13].

Table 1
CAS used for MRCI calculation, the optimized distance (d_{opt}) of the dimer system and its interaction energy (E_{int}).

Dimer	CAS	d_{opt} (Å)	E_{int} (kcal/mol)
$[Eu–OH_2]^{2+}$	$8a_1\ 9a_1\ 4b_1\ 5b_1\ 6b_1\ 7b_1\ 5b_2\ 6b_2\ 2a_2$	2.427	−47.32
$[La–OH_2]^{3+}$	$4b_1\ 5b_1\ 6b_1\ 7b_1$	2.315	−91.84
$[Eu–OH_2]^{3+}$	$8a_1\ 4b_1\ 5b_1\ 6b_1\ 7b_1\ 5b_2\ 6b_2\ 2a_2$	2.197	−107.80
$[Gd–OH_2]^{3+}$	$8a_1\ 9a_1\ 4b_1\ 5b_1, 6b_1\ 7b_1\ 5b_2\ 6b_2\ 2a_2$	2.191	−108.41
$[Lu–OH_2]^{3+}$	$6b_1\ 7b_1, 8b_1$	2.100	−118.90
$[Ac–OH_2]^{3+}$	$4b_1\ 5b_1, 6b_1\ 7b_1\ 8b_1$	2.427	−84.30
$[Am–OH_2]^{3+}$	$8a_1\ 4b_1\ 5b_1\ 6b_1\ 7b_1\ 5b_2\ 6b_2\ 2a_2$	2.270	−102.19
$[Cm–OH_2]^{3+}$	$8a_1\ 9a_1\ 4b_1\ 5b_1\ 6b_1\ 7b_1\ 5b_2\ 6b_2\ 2a_2$	2.255	−108.41
$[Lr–OH_2]^{3+}$	$6b_1\ 7b_1, 8b_1$	2.163	−111.75
$[Th–OH_2]^{4+}$	$4b_1\ 5b_1\ 6b_1\ 7b_1$	2.218	−160.40

3. Results and discussion

3.1. Large core decomposition

Table 2 gives the energy decomposition analysis of the different dimers at their optimized geometry with a large core pseudopotential. E_1 is the first order energy, i.e. the sum of the electrostatic term and exchange-repulsion. The order of magnitude of this contribution mainly depends on the charge of the system as well as on the atomic number. However, all the large-core pseudopotentials were designed to have only eight valence electrons, but should be able to account for the increasing number of electrons from Lanthanum to Lawrencium. Indeed, a general trend in the first order energies can be observed among the trivalent cations of both series as the atomic number increases: Ln(III): La < Eu < Gd < Lu; An(III): Ac < Am < Cm < Lr. Also, another trend down the same column is present, meaning that for a given configuration of valence electrons e.g. nf^6 or nf^7, the increase in the number of core electrons is still taken into account by the pseudopotential. However in relative percentage of E_1, the cations are arranged quite differently across both series: Ln(III): Eu < Gd < La < Lu; An(III): Am < Cm < Lr < Ac. This new trend highlights the difference between the open and closed shell cations: indeed, it seems that the contribution of the first order energy is somewhat weaker in the open shell cations, indicating that the ionic degree of the bond is less than in the closed shell systems. In the case of the $4f^0$ and $4f^{14}$ lanthanide cations, the La(III) system features a smaller E_1 contribution than Lu(III) which is expected with respect to the increasing Z number. On the other hand, across the actinide series, the $5f^0$ Ac(III) cation is clearly more ionic than the $5f^{14}$ Lr(III) cation. The Lawrencium(III) cation however is found to show a different behavior than the other f-elements, due to its completely filled 5f shell and smaller ionic radius.

Concerning the polarization energies, the relative percentage of the value with respect to the total interaction energy is found to account for approximately 50%. Since the polarization energy depends on the charge of the system, the contribution for the Eu(II) divalent cation adds up to 40% while that of the tetravalent actinide Th(IV) rises to more than 60%. Still, in all the trivalent systems, the values of this contribution are greater than the frozen core (E_1). The different cations of each series can be defined in term of the increasing relative percentage of the polarization energies: Ln(III):

Table 2
Large core pseudopotential energy decomposition analysis of the mono aqua complexes of the different f-cations arranged in increasing Z number. All energies are in kcal/mol.

Dimer	d_{opt} (Å)	E_1	POL	CT	E_{int}	%POL	%CT
$[Eu–OH_2]^{2+}$	2.427	−21.18	−17.69	−4.26	−43.73	40.46	9.74
$[La–OH_2]^{3+}$	2.315	−24.48	−44.41	−10.97	−82.31	53.95	13.32
$[Eu–OH_2]^{3+}$	2.197	−26.34	−49.77	−14.67	−93.69	53.12	15.65
$[Gd–OH_2]^{3+}$	2.191	−27.88	−50.01	−14.69	−95.42	52.41	15.39
$[Lu–OH_2]^{3+}$	2.100	−32.50	−55.03	−17.16	−107.72	51.09	15.93
$[Ac–OH_2]^{3+}$	2.427	−26.74	−39.44	−6.62	−74.58	52.88	8.87
$[Am–OH_2]^{3+}$	2.270	−28.71	−45.87	−11.15	−88.17	52.02	12.65
$[Cm–OH_2]^{3+}$	2.255	−29.70	−46.50	−11.52	−90.19	51.56	12.77
$[Lr–OH_2]^{3+}$	2.163	−34.64	−51.70	−13.47	−102.52	50.42	13.14
$[Th–OH_2]^{4+}$	2.218	−26.23	−86.96	−17.99	−136.75	63.59	13.16

Table 3
Comparison of the large core (lc) and small core (sc) values of the frozen core energy (E_1), the induction energy (E_2), the polarization energy of the metal cation (POLB) and the interaction energies of the mono aqua complexes as calculated within the CSOV framework. All given values are in kcal/mol. NC = not converged.

Dimer	E_1		E_2		POL_B		E_{int}	
	sc	lc	sc	lc	sc	lc	sc	lc
$[Eu–OH_2]^{2+}$	−22.75	−21.18	−22.12	−22.55	−0.79	−0.60	−44.87	−43.73
$[La–OH_2]^{3+}$	−25.77	−24.48	−60.01	−57.83	−1.47	−1.21	−85.78	−82.31
$[Eu–OH_2]^{3+}$	N.C.	−26.34	N.C	−67.35	N.C	−1.11	N.C.	−93.69
$[Gd–OH_2]^{3+}$	−30.10	−27.88	−67.82	−67.54	−1.55	−1.06	−97.91	−95.42
$[Lu–OH_2]^{3+}$	−34.89	−32.50	−74.54	−75.22	−0.92	−0.92	−109.43	−107.72
$[Ac–OH_2]^{3+}$	−27.35	−26.74	−49.60	−47.85	−1.40	−1.18	−76.95	−74.58
$[Am–OH_2]^{3+}$	N.C	−28.71	N.C.	−59.46	N.C	−1.17	N.C.	−88.17
$[Cm–OH_2]^{3+}$	−29.52	−29.70	−63.28	−60.49	−2.36	−1.14	−92.80	−90.19
$[Lr–OH_2]^{3+}$	−26.72	−34.64	−78.69	−67.88	−1.68	−0.98	−105.41	−102.52
$[Th–OH_2]^{4+}$	−27.40	−26.23	−118.78	−110.51	−2.40	−2.00	−146.18	−136.75
$[Th–OH_2]^{4+}$[a]		−23.06		−115.09		−2.58		−145.47

[a] CRENBL large core pseudopotential.

La < Eu < Gd < Lu; An(III): Ac < Am < Cm < Lr. The trend is the same one that is followed by the frozen energy component and was to be expected.

Lastly, the charge transfer term is seen to be a non-negligible contribution, accounting for about 15% of the total interaction energy. It is of course, clearly dependent on the optimized bond length**.** Indeed, regardless of the charge, the relative percentage of total charge transfer in the system is a function of the optimized bond length: for shorter bond lengths,%CT increases.

A table summarizing these values can be found in Supporting Information. Also, if considering only the trivalent cations, the ligand–metal charge transfer ($CT_{B->A}$) also follows the same trend. The mixing of orbitals at shorter bond lengths is probably enhanced and would allow for partial electron transfer between the ligand and the vacant orbitals in the metal.

However it must be kept in mind that this study was carried out with a large core pseudopotential which does not feature explicit f-orbitals or electrons. Therefore, in order to support all the results, the small core pseudopotential EDA was much called for at this point.

3.2. Small core decomposition

The results of the small core energy decomposition analysis are summarized in Table 3. Besides investigating the importance of the charge transfer term from the ligand (fragment A) to the metal (fragment B) with a higher number of valence electrons, the contribution of the unpaired electrons to the polarization energy term of the cation was also addressed. This contribution, as mentioned earlier is the most interesting to us as a pure polarization energy curve is required for the development of polarizable force fields for lanthanides and actinides. This study will therefore focus on evaluating the accuracy of the large core pseudopotential polarization curve as compared with the more physically relevant and precise small core curve, namely in the case of the open shell systems (see Table 4). All three cations in the table have the same outermost electron shell configuration, namely a half filled f-orbital. Despite being open shell, those systems are mono reference and extra stable. On the other hand, the nf^6 configurations of Eu(III) and Am(III) generate several configurations for the ground state. As a result, the wavefunction could not be converged based on the mono determinant approximation used in the MCSCF approach of HONDO.

Table 4
Polarization energy of unpaired electrons ($Pol_{é}$) of the open shell cations in kcal/mol and their percentage contribution (%) to the polarization energy of the cation.

d_{M-Ow} (Å)	Eu(II)		Gd(III)		Cm(III)	
	$Pol_{é}$	%	$Pol_{é}$	%	$Pol_{é}$	%
1.8	−1.647	16.5	−2.442	29.0	−7.104	40.8
1.9	−0.975	15.9	−1.516	29.1	−4.414	41.2
2.0	−0.593	15.4	−0.962	28.8	−2.810	41.5
2.1	−0.369	14.7	−0.621	28.2	−1.826	41.6
2.2	−0.233	13.7	−0.407	27.2	−1.208	41.3
2.3	−0.150	12.6	−0.270	25.9	−0.810	40.6
2.4	−0.098	11.4	−0.182	24.5	−0.551	39.6
2.5	−0.065	10.2	−0.123	22.8	−0.378	38.1
2.6	−0.043	8.9	−0.084	21.1	−0.262	36.3
2.7	−0.029	7.7	−0.057	19.0	−0.182	34.1
2.8	−0.020	6.7	−0.039	17.0	−0.128	31.9
2.9	−0.014	5.9	−0.027	15.2	−0.089	29.2
3.0	−0.014	7.2	−0.018	12.9	−0.063	26.7
3.1	−0.007	4.5	−0.012	10.8	−0.044	23.9
3.2	−0.005	3.9	−0.008	9.0	−0.031	21.4
3.3	−0.003	2.9	−0.006	8.2	−0.021	18.3
3.4	−0.002	2.3	−0.004	6.8	−0.015	16.1
3.5	−0.002	2.8	−0.003	6.1	−0.010	13.3
3.6	−0.001	1.7	−0.002	4.9	−0.007	11.3
3.7	−0.001	2.0	−0.001	2.9	−0.005	9.6
3.8	−0.001	2.3	−0.001	3.4	−0.003	7.0

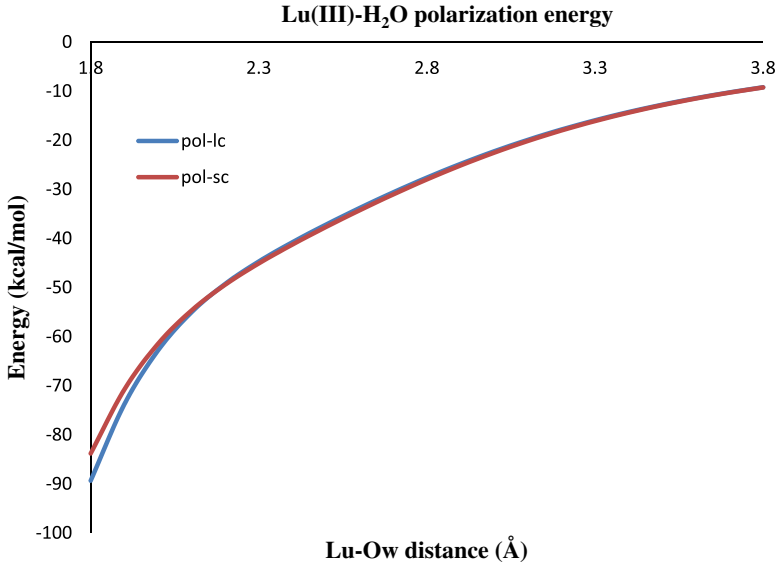

Figure 1. Polarization energy of the $[Lu–OH_2]^{3+}$ dimer systems as calculated with both a small and large core pseudopotential as a function of the Lu–O_w distance. As in the general case, a good agreement is observed between small and large core pseudopotentials.

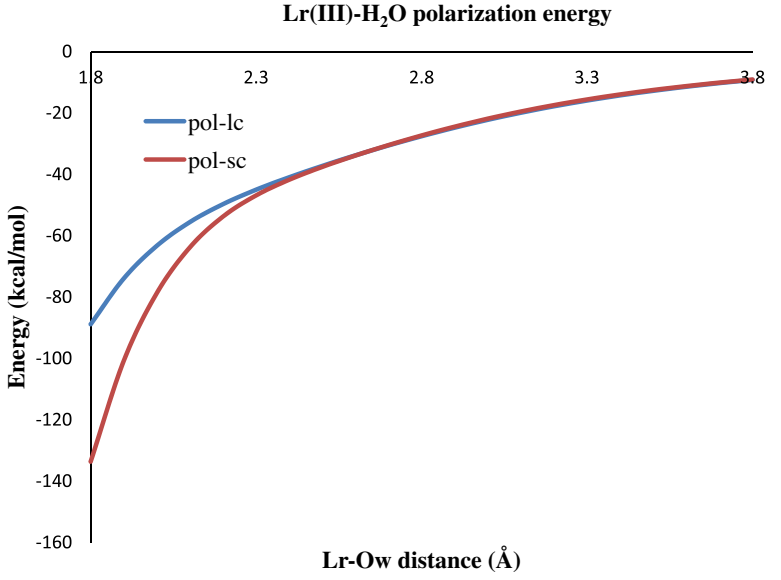

Figure 2. Polarization energy of the $[Lr–OH_2]^{3+}$ dimer systems as calculated with both a small and large core pseudopotential as a function of the Lr–OH_2 distance. Differences are observed at short range between small and large core pseudopotentials.

The contribution of the polarization energy of the unpaired electrons is clearly non negligible, as it accounts for more than 10% of the cations' polarization energy, around the different optimized bond lengths i.e. from 2.0 to 2.5 Å. Concerning the closed shell cations (see Figures 1 and 2), both the small and large core pseudopotentials yields the same polarization energy curves except for Lawrencium which is given as Figure 2. The difference in the polarization energy as calculated with the small or large core pseudopotential sums up to 8.2 kcal/mol out of the small core polarization energy of −63.8 kcal/mol. Furthermore, when analyzing the values relative to Lr(III) in Table 3, it seems that the behavior of the Lr(III) ion is very different compared to that of the all the reported cations. Indeed, the Lawrencium cation features a completely filled 5f shell and is the heaviest of all the studied cations. This might give rise to a physical and/or chemical behavior that is both unexpected and very different than that which was known of the lighter lanthanides and actinides.

Overall, we noticed a good agreement between small and large core EDA results. Nevertheless, one exception should be raised: the Th(IV) mono aqua complex. In this particular case, there is a 10 kcal/mol discrepancy between the two types of pseudopotentials used. However, in our previous work on Th(IV) [21], we used the large core CRENBL [32] which gave results more in line with Dolg's small core energy values. Therefore, one could be cautious about the use of large core pseudopotentials for + IV heavy metal cations that probably embody too few basis functions in order to be used with a triple zeta + difuse functions basis set for water.

4. Conclusion

Nonetheless, the behavior of all the different contributions to the interaction energy is quite similar when computed either with the small or large core pseudopotential in general. We are thus

comforted in the fact that scalar relativistic large core pseudopotentials can be used to estimate the polarization contribution that is required for force field development. Nevertheless, our results show that, in certain cases, it could be important to explicitly treat the open-shell polarization contribution, namely in the case of the open-shell cations for a more accurate and physically relevant polarization energy curve. Such findings are consistent with the already discussed potential deficiencies of large core pseudopotentials for f elements pointed out in the Literature (see discussion on Refs. [33–35] and references therein) that concern the lack of static and dynamic core polarization. In the context of our work, i.e. the computation of total interactions energies aimed to design new force fields for f-elements, such limitations can be accepted as differences are minimal despite the fact that potential error compensation could occur (one should keep in mind that more important deviations between small and large core could affect the quality of the computation of other types of properties).

The obvious next step will be to perform these calculations at a correlated level, which would require a thorough study of CASSCF active spaces or density functionals so as to determine the one which is more adapted to the study of heavy metals. Two peculiar comportments were noticed for the Lawrencium and Thorium cations.

To conclude, this work also opens the possibility to extend the ab initio parameterization of polarizable force fields for lanthanides and actinides beyond closed-shell complexes [18,21] which will enable the tackling of open-shell ones (Marjolin et al., in preparation). Future work going beyond the inclusion of non-dynamical correlation at the MCSCF level will be necessary to explicitly include the 'dynamical' dispersion effects within EDA computations (CASPT2, MRCI etc. . .). As we observed strong charge transfer contributions, additional complexities will be encountered while computing the PES of several of these mono aqua complexes. Indeed, state crossings corresponding to the ionization of the water molecule do exist and will require a special attention within future EDA procedures.

Appendix A. Supplementary data

Supplementary data associated with this article can be found, in the online version, at http://dx.doi.org/10.1016/j.cplett.2013.01.066.

References

[1] A.E. Merbach, E. Toth, The Chemistry of Contrast Agents in Medical Magnetic Resonance Imaging, Wiley, Chichester, 2001.
[2] L.K. Nicholas, N.J. Long, Chem. Soc. Rev. 35 (2006) 557.
[3] E.G. Moore, A.P.S. Samuel, Acc. Chem. Res. 42 (2009) 542.
[4] Z.M. Hou, Coord. Chem. Rev. 231 (2002) 1.
[5] R. Silva, H. Nitsche, Radiochim. Acta 70 (1995) 377.
[6] I. Grenthe, J. Fuger, R. Konings, R. Lemire, A. Muller, C. Nguyen-Trung, H. Wanner, in: H. Wanner, I. Forest (Eds.), Chemical Thermodynamics of Uranium, North-Holland, Amsterdam, 1992.
[7] K.L. Nash, C. Madic, J.N. Mathur, Actinide separation science and technology, in: L.R. Morss, N.M. Edelstein, J. Fuger (Eds.), The Chemistry of the Actinide and Transactinide Elements, Springer, Dordrecht, 2006.
[8] C. Gourlaouen, J.-P. Piquemal, T. Saue, O. Parisel, J. Comput. Chem. 27 (2006) 142.
[9] C. Gourlaouen, J.-P. Piquemal, O. Parisel, J. Chem. Phys. 124 (2006) 174311.
[10] C. Gourlaouen, O. Parisel, J.-P. Piquemal, Chem. Phys. Lett. 469 (2009) 38.
[11] C. Gourlaouen, O. Parisel, J.-P. Piquemal, J. Chem. Phys. 133 (2010) 124310.
[12] P.S. Bagus, K. Herman, C.W. Bauschlicher Jr., J. Chem. Phys. 81 (1984) 1966.
[13] C.W. Bauschlicher, P.S. Bagus, C.J. Nelin, B.O. Roos, J. Chem. Phys. 85 (1986) 354.
[14] J.-P. Piquemal, A. Marquez, C. Giessner-Prettre, J. Comput. Chem. 26 (2005) 1052.
[15] N. Gresh, G.A. Cisneros, T.A. Darden, J.-P. Piquemal, J. Chem. Theory Comput. 3 (2007) 1960.
[16] C. Clavaguéra, J.-P. Dognon, Chem. Phys. 311 (2005) 169.
[17] R. Pollet, C. Clavaguéra, J.-P. Dognon, J. Chem. Phys. 124 (2006) 164103.
[18] F. Réal, V. Vallet, C. Clavaguéra, J.-P. Dognon, Phys. Rev. A 78 (2008) 052502.
[19] J. Wu, J.-P. Piquemal, R. Chaudret, P. Reinhardt, P. Ren, J. Chem. Theory Comput. 6 (2010) 2059.
[20] J.-P. Piquemal, L. Perera, G.A. Cisneros, P. Ren, L.G. Pedersen, T.A. Darden, J. Chem. Phys. 125 (2006) 054511.
[21] A. Marjolin et al., Theor. Chem. Acc. 131 (2012) 1198.
[22] K. Kitaura, K. Morokuma, Int. J. Quantum Chem. 10 (1976) 325.
[23] M. Dupuis, A. Marquez, E.R. Davidson, HONDO95.3, Quantum Chemistry Program Exchange (QCPE), Indiana University, Bloomington, IN 47405.
[24] H.J. Werner et al. MOLPRO, version 2008.1; University of Stuttgart and Birmingham, Germany and Great Britain, 2008.
[25] T.H. Dunning Jr., J. Chem. Phys. 90 (1989) 1007.
[26] M. Dolg, H. Stoll, H. Preuss, J. Chem. Phys. 90 (1989) 1730.
[27] (a) M. Dolg, H. Stoll, A. Savin, H. Preuss, Theor. Chim. Acta 75 (1989) 173; (b) X. Cao, M. Dolg, J. Chem. Phys. 115 (2011) 7348.
[28] (a) X. Cao, M. Dolg, J. Mol. Struct. 581 (2002) 139; (b) X. Cao, M. Dolg, H. Stoll, J. Chem. Phys. 118 (2003) 487.
[29] X. Cao, M. Dolg, J. Mol. Struct. 673 (2004) 203.
[30] A. Moritz, X. Cao, M. Dolg, Theor. Chem. Acc. 117 (2007) 473.
[31] A. Moritz, X. Cao, M. Dolg, Theor. Chem. Acc. 118 (2007) 845.
[32] W.C. Ermler, R.B. Ross, P.A. Christiansen, Int. J. Quantum Chem. 40 (1991) 829.
[33] C. Clavaguéra, F. Calvo, J.-P. Dognon, J. Chem. Phys. 124 (2006) 074505.
[34] C. Clavaguéra, E. Sansot, F. Calvo, J.-P. Dognon, J. Phys. Chem. B 110 (2006) 12848.
[35] C. Clavaguéra, R. Pollet, J.M. Soudan, V. Brenner, J.-P. Dognon, J. Phys. Chem. B 109 (2005) 7614.